ACS OMEGA

Open Access

http://pubs.acs.org/journal/acsodf

Article

Arabidopsis Dph4 is an Hsp70 Cochaperone with Iron-Binding Properties

Amit Kumar Verma,[#] Priya Sharma,[#] Zeyaul Islam,[*] Anup Kumar Biswal, Yogesh Tak, and Chandan Sahi[*]

Cite This: *ACS Omega* 2024, 9, 37650−37661

Read Online

ACCESS | Metrics & More | Article Recommendations | Supporting Information

ABSTRACT: J-domain proteins (JDPs) are obligate cochaperones of Hsp70s with a wide range of functions in protein homeostasis. Although the J-domain is required for the stimulation of Hsp70s ATPase activity, the functional specificity of JDPs is governed by domains or regions other than the J-domain. Jjj3/Dph4, a class III JDP, is required for diphthamide (DPH) biosynthesis in eukaryotes, including yeast and mammals. Dph4 has a conserved N-terminal J-domain and an uncharacterized C-terminal domain containing a signature CSL zinc finger motif. Previously, we showed that the Dph4 ortholog in *Arabidopsis thaliana* (atDjC13/*At*Jjj3/*At*Dph4) could restore DPH biosynthesis in yeast *jjj3*Δ mutant in a J-domain-dependent manner. Here, we characterize the C-terminal CSL motif of *At*Dph4 using yeast genetic and biochemical approaches. The CSL motif of *At*Dph4 is essential for DPH biosynthesis, and like human Dph4, *At*Dph4 showed distinct iron-binding activity, which is not present in its yeast counterpart. *Sc*Dph4 and *At*Dph4 proteins exhibit distinct iron-binding capabilities, as evidenced by UV−vis spectrophotometry, SEM-EDS (energy-dispersive spectroscopy function on the scanning electron microscope) and electron paramagnetic resonance (EPR) spectra analyses. Collectively, our data suggests that beyond their role as an Hsp70 cochaperone, Dph4 homologues in complex eukaryotes may have iron-binding abilities, indicating a potential role in iron-sulfur cluster assembly and iron homeostasis.

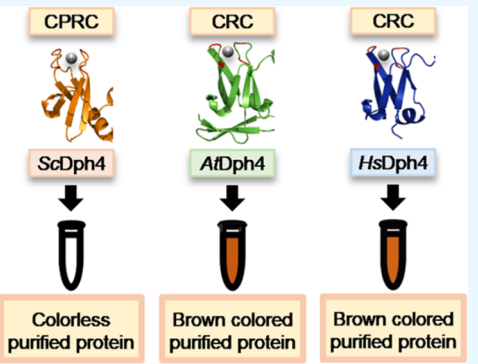

INTRODUCTION

Proteins undergo a variety of post-translational modifications (PTMs) that affect their functions, localization, solubility, assembly, folding, interactions with nucleic acids, lipids, and other proteins, as well as their degradation.[1−3] Among the several known PTMs that occur on multiple amino acids in different proteins, one exceptional modification is diphthamide (DPH), which is restricted to a single amino acid of a single protein in the entire proteome.[4−6] DPH is a highly conserved and unique post-translational modification found in domain IV of eukaryotic Elongation Factor 2 (eEF2).[5,6] Based on ribosomal frame-shift assays from the structural and functional yeast mutants, DPH is proposed to be essential for the maintenance of translational fidelity and the rate of translational elongation.[7−11] Paradoxically, DPH can be ADP-ribosylated by bacterial toxins including Diphtheria toxin (DT) from *Corynebacterium diphtheriae*, Exotoxin A (ETA) from *Pseudomonas aeruginosa*, and Cholix toxin (ChxA) from *Vibrio cholerae*, resulting in a nonfunctional eEF2 that halts translation.[12−15]

DPH biosynthesis is a four-step process involving multiple proteins (Dph1-7, Kti11; Figure 1). In the first step, a 3-amino-3-carboxypropyl (ACP) radical is transferred from S-Adenosyl methionine (SAM) to the C2 position of the critical histidine residue in eEF2, leading to the formation of an ACP-modified eEF2 intermediate, catalyzed by Dph1-4 enzymes (Figure 1).[16,17] Dph1-3 forms a multimeric protein complex, where Dph1 and 2 catalyze ACP transfer and Dph3 serves to channel electrons to the iron-sulfur clusters of Dph1 and Dph2 proteins, maintaining their redox state.[16,17]

Dph4 (DPH biosynthesis 4) or Jjj3 is a J-domain protein (JDP) that plays an essential but still elusive role in the first step of DPH biosynthesis in budding yeast (Figure 1).[18,19] Although nonessential in budding yeast, Dph4 is essential for normal growth and development in more complex eukaryotes. Homozygous mouse mutants display growth retardation, developmental delay, embryonic lethality, preaxial polydactyly, and neurodegeneration.[20] Dph4 is also implicated in apoptosis and signaling.[21,22] *jjj3/dph4* knockout yeast cells are sensitive to a range of drugs and compounds, including rapamycin, caffeine, hygromycin B, cycloheximide, and wortmannin.[23−25] JDPs are highly diverse cochaperones of Hsp70s that promote protein folding, assembly and disassembly of protein

Received: February 23, 2024
Revised: July 6, 2024
Accepted: July 30, 2024
Published: August 28, 2024

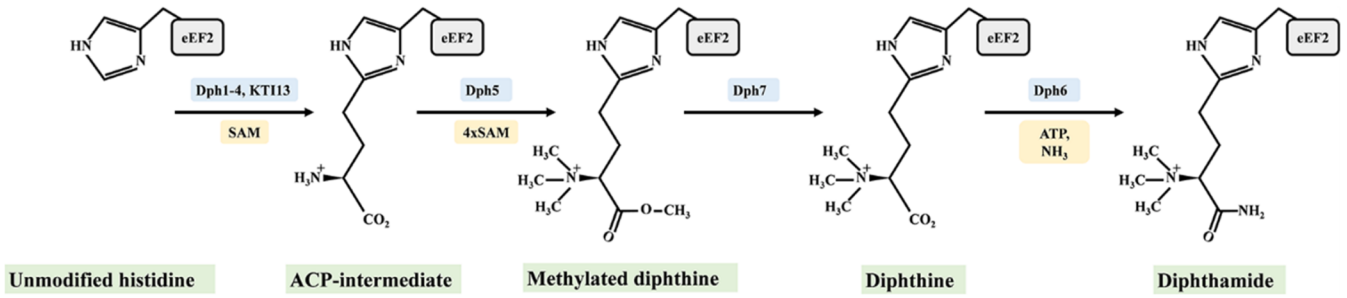

Figure 1. Diphthamide biosynthesis pathway in eukaryotes. Diphthamide biosynthesis requires at least eight proteins (Dph1-7 and Kti13). The biosynthesis starts with the conversion of unmodified histidine to an ACP-intermediate that requires Dph1-4 proteins and the Kti13 protein. The intermediate then undergoes tetra methylation by Dph5 in the second step of the pathway, generating methylated diphthine. Dph7 then demethylates methylated diphthine, leading to the formation of diphthine, which is a substrate for the final enzyme of the pathway. Dph6 catalyzes the ATP-driven amidation of diphthine using ammonia as a source of the amide group, yielding diphthamide.

structures, transport of proteins within the cell, and degradation of misfolded, unstable, and aggregated proteins.[26−28] All JDPs have a characteristic J-domain containing a conserved HPD (Histidine-Proline-Aspartate) tripeptide motif in a loop between helices II and III that is essential for the stimulation of the otherwise poor ATPase activity of Hsp70s.[26,28,29] While the J-domain is essential for all Hsp70 cochaperone functions of JDPs, functional specificity of JDPs emerges from domains/regions outside the J-domain.[26,27,30]

JJJ3/Dph4 possesses an N-terminal J-domain and a CSL-type zinc finger motif at the C-terminal that consists of four conserved cysteine residues (Cys-X-Cys···Cys-X2-Cys), which tetrahedrally can coordinate both Zinc (Zn) and Iron (Fe). The last cysteine residue is followed by serine (S) and a leucine (L) residue, hence the name "zf-CSL" from the CSL tripeptide.[19,31,32] The domain comprises a three-stranded β-sandwich with one sheet consisting of two parallel strands (β1 and β6) and one antiparallel strand (β5). The second sheet consists of three strands (β2, β3, and β4) running antiparallel to each other. A short α-helix separates the two sheets.[31] The J-domain and a CSL domain are connected with a flexible linker region that maintains the structural integrity of the two domains and allows them to perform independent functions.[31] Both mammalian (*Hs*Dph4) and *Arabidopsis thaliana* (*At*Dph4) orthologs can substitute for *Sc*Dph4, for DPH biosynthesis in budding yeast suggesting conservation of function.[31,33] Furthermore, for their function in DPH biosynthesis, *Sc*Dph4 and its mammalian and plant counterparts require both their J-domain as well as the CSL zinc finger motif.[31,33,34]

Human Dph4 protein binds to both zinc and iron with its C-terminal CSL motif.[31] However, it predominantly exists in an iron-bound state, as Fe-Dph4 has a better ability to stimulate the ATPase activity of Hsp70 compared with Zn-Dph4 under similar conditions.[31] Fe-Dph4 has redox and electron carrier activity; it undergoes oligomerization, thus acting as a transient iron reservoir to maintain iron homeostasis.[31] Interestingly, *Sc*Dph4 neither binds to iron nor donates electrons to the Fe−S cluster of the Dph1-2 heterodimer.[32] Thus, Dph4's role in the first step of the DPH pathway awaits further study. Previously, we reported the presence of the Dph4 ortholog, viz., *At*Dph4, in *A. thaliana* and showed that *At*Dph4 could restore DPH biosynthesis in the *jjj3*Δ mutant of budding yeast.[33] In the study presented here, we show that the C-terminal CSL motif of atDjC13/*At*Dph4 is crucial for DPH biosynthesis. Biochemical studies reveal that, like its mammalian orthologs, *At*Dph4 also binds iron, a property also shared by Dph3, another protein having a crucial redox-active function in DPH biosynthesis.[32] Using chimeric constructs, we show that *At*Dph4 is a highly specialized JDP that has two distinct activities. Through its J-domain, it works as an Hsp70 cochaperone, and its iron-binding CSL zinc finger motif has redox activity of unknown significance.

MATERIALS AND METHODS

In-Silico Methods. Dph4 orthologs in various organisms were identified by BLASTP searches in NCBI (https://blast.ncbi.nlm.nih.gov/Blast.cgi?PAGE=Proteins) and their specific databases, e.g., Saccharomyces Genome Database (https://www.yeastgenome.org/blast-sgd) for fungal species and the TAIR (https://www.arabidopsis.org/Blast/index.jsp)[35−37] database for *A. thaliana* using *Sc*Dph4 as the query sequence. The top results with a significantly high score and low E-value were shortlisted and used to perform the "reverse BLAST" in SGD. Those sequences that resulted in the Dph4 protein were considered Dph4 orthologs.[38] Multiple sequence alignment was done using MAFFT (https://mafft.cbrc.jp/alignment/server/),[39] and alignment of the secondary structure was done using ESpript3 (https://espript.ibcp.fr/ESPript/cgi-bin/ESPript.cgi).[40] These orthologs were then examined for the presence of distinct domains and motifs using domain prediction at the NCBI Conserved Domain Database (CDD, Batch CD-search) (https://www.ncbi.nlm.nih.gov/Structure/bwrpsb/bwrpsb.cgi).[41] The IBS (Illustrator of Biological Sequences)[42] tool was used to create the schematic representations. The tertiary structures were predicted with the α fold protein structure database (https://alphafold.ebi.ac.uk/)[43] and visualized with PyMol (The PyMOL Molecular Graphics System, Version 2.0, Schrödinger, LLC.).

Yeast Methods. The yeast genes (*Sc*Dph3 and *Sc*Dph4) were amplified by PCR from genomic DNA isolated from the diploid BY4741 strain. The *A. thaliana DPH4* gene was amplified using specific primer pairs (Table S1) using *Arabidopsis* cDNA. Point mutations were generated using the site-directed mutagenesis technique.[44] Dph4 and Dph3 chimera constructs were made using the PCR sewing method[45] in the *HIS*-based marker plasmid pRS413.[46] All constructs are listed in Table 1. For assessing DPH biosynthesis in yeast cells, their sensitivity to DT was monitored. Constructs were double transformed with a *URA3*-marked *GAL*-DT plasmid in *dph4*Δand *dph3*Δyeast strains using the LiAc/SS carrier DNA/PEG method.[47] The functionality was tested by

https://doi.org/10.1021/acsomega.4c01776
ACS Omega 2024, 9, 37650−37661

Table 1. List of Plasmid Constructs Used in the Study

plasmid	gene	base vector	source
pCS944	*Sc*Dph4	pRS413-*TEF*	this study
pCS68	*Sc*Dph4	pRS414-*TEF*	this study
pCS1073	*Ca*Dph4	pRS414-*TEF*	this study
pCS1074	*Kl*Dph4	pRS414-*TEF*	this study
pCS977	*At*Dph4	pRS413-*TEF*	this study
pCS1101	*At*Dph4	pRS414-*TEF*	this study
pCS1076	*Hs*Dph4	pRS414-*TEF*	this study
pCS1103	$AtDph4_{H39Q}$	pRS414-*TEF*	this study
pCS1102	$AtDph4_{C158Y}$	pRS414-*TEF*	this study
pCS945	*Sc*Dph4_P114A	pRS413-*TEF*	this study
pCS946	*Sc*Dph4_del: P114	pRS413-*TEF*	this study
pCS947	*Sc*Dph4_C152A	pRS413-*TEF*	this study
pCS941	*Sc*Dph4_C113A	pRS414-*TEF*	this study
pCS1104	*At*Dph4_add:113P	pRS414-*TEF*	this study
pCS1106	*At*Dph4_C114A	pRS414-*TEF*	this study
pCS1107	*At*Dph4_C155A	pRS414-*TEF*	this study
pCS13	*At*Dph4-C	pRS413-*TEF*	this study
pCS1096	*Sc*Dph3	pRS413-*TEF*	this study
pCS1099	*Sc*Dph4-J+ *Sc*Dph3	pRS413-*TEF*	this study
pCS1100	*Sc*Dph4-J+ *At*Dph4-C	pRS413-*TEF*	this study
pCS77	Gal-DT	pYES2	Thakur et al.[31]
pCS172	empty vector	pRS314	Sahi and Craig[34]
pCS210	*Sc*Dph4	pET28a	this study
pCS213	*At*Dph4	pET28a	this study
pCS1299	*At*Hsp70-1	pSMT3	this study
pCS1535	*At*Hsp70-14	pSMT3	this study

monitoring yeast growth on conditional expression of *GAL-DT* in a galactose-containing medium. The CDS of *At*Hsp70-1 (Hsc70-1) and *At*Hsp70-14 (NEF) were amplified from *Arabidopsis* cDNA (Table S1) and cloned in *Bam*HI /*Xma*I sites of pSMT3 vector (Table 1) (Mossessova and Lima).[72]

Western Analysis. Western analysis was performed as described in ref 33. Briefly, an equal number of cells in the exponential phase were used to isolate the total protein. The cells were treated with 0.1 M NaOH before being resuspended in SDS sample buffer (62.5 mM Tris HCl, pH 6.8, 5% glycerol, 2% SDS, 2% β-mercaptoethanol, and 0.01% bromophenol blue). To detect protein, anti-Dph4 or anti-HA (Sigma-Aldrich) rabbit antibodies were used. Image Quant software (Molecular Dynamics, Sunnyvale, CA) was used for quantification.

Protein Expression and Purification. All Dph4 proteins were overexpressed in*Escherichia coli* Rosetta cells at an OD_{600} of 0.6−0.8, with IPTG (0.25 mM) and an O/N incubation at 16 °C and 200 rpm. His-tagged proteins were purified using immobilized metal affinity chromatography (IMAC) with Ni-NTA resin. For purification, the cells were resuspended in lysis buffer (50 mM Tris pH 8.0, 150 mM NaCl, 10% Glycerol, 1 mM DTT) and incubated on ice for 30 min with the addition of lysozyme, 1 mM PMSF, and a protease inhibitor cocktail (Sigma-Aldrich). Cells were then lysed by sonication (45% amplitude, 10s O/N, 20s OFF, 10 min). The lysate was then clarified by centrifugation at 15,000 rpm at 4 °C for 30 min. The supernatant was incubated for an hour with the Ni-NTA resin (Qiagen, Cat. No. 30210) at 4 °C. After passing the flow-through, the beads were washed with the lysis buffer thrice, and finally, His-tagged protein was eluted in 1 mL fractions using an imidazole gradient (50 mM Tris pH 8.0. 150 mM NaCl, 10% Glycerol, 1 mM DTT) with imidazole salt ranging from 250 to 600 mM. Protein-elution fractions were concentrated using MF-Millipore membrane filters with a pore size of 10 kDa. The aliquots were flash-frozen in liquid nitrogen and stored at −80 °C. Polyclonal anti-*At*Dph4 antibodies were raised against full-length 6xHis-*At*Dph4 protein in CD-1 mice in the animal facility of IISER Bhopal.

*At*Hsp70-1-pSMT3 and *At*Hsp70-14-pSMT3 constructs were overexpressed in Rosetta cells. Protein expression was induced at OD_{600} 0.8 using 0.5 mM IPTG at 16 °C for 20 h. The cells were harvested by centrifugation at 6,000 *g* for 10 min. Cells were resuspended in lysis buffer (50 mM Tris pH7.5, 100 mM KCl, 0.5% triton X-100, 1 mM PMSF, 0.5 mM DTT, 20 mM imidazole, and 1 mg/mL lysozyme) and incubated at ice temperature for 30 min. The cells were sonicated for complete lysis using a probe sonicator. The lysate was centrifuged at 16,000 *g* for 30 min. The supernatant was incubated with Ni-NTA agarose beads for 3 h at 4 °C. Flow-through was collected, and Ni-NTA beads were washed in wash buffer 1 (50 mM Tris pH7.5, 100 mM KCl, 0.5% triton X-100, 1 mM PMSF, 0.5 mM DTT, and 20 mM imidazole) and wash buffer 2 (50 mM Tris pH7.5, 100 mM KCl, 0.5% triton X-100, 1 mM PMSF, 0.5 mM DTT, and 30 mM imidazole). For *At*Hsp70-1, the bound protein was incubated with 2 units of alkaline phosphatase (per mg of bound protein) for 10 min at room temperature and then washed, additionally, with wash buffer 2. Bound protein was eluted in an elution buffer (50 mM Tris (pH 7.5), 100 mM KCl, and 250 mM imidazole). The eluted protein was dialyzed against a dialysis buffer (50 mM Tris pH 7.5, 100 mM KCl, 500 μM DTT, 1 mM $MgCl_2$) in the presence of SENP1 (Ulp protease) for 12 h. The cleaved tag was bound to the Ni-NTA agarose beads for 2 h at 4 °C, and the protein without tag was collected as flow-through.

ATPase Assay. About 0.5 μM purified Hsp70 (*At*Hsp70-1) was incubated with 8 μM Hsp40 (*At*Dph4 or $AtDPH_{H39Q}$) and NEF (*At*Hsp70-14) in ATPase assay buffer (50 mM Tris, pH 7,5; 100 mM KCl, 500 μM DTT) with 1 mM ATP. Also, 50 μL of the reaction mixture was transferred to a 96-well plate in triplicate, which was incubated at 25 °C. To each well, 150 μL of malachite green reagent mix (0.081% (w/v) malachite green in 6N H_2SO_4, 5.7% ammonium heptamolybdate in 6 N HCl, and 0.7% (w/v) poly(vinyl alcohol) in water; all in 2:1:3 ratio) was added and incubated for 10 min at room temperature before stopping the reaction with 3.7% trisodium citrate. The absorbance was recorded at 620 nm in a plate reader (Eon microplate spectrophotometer, BioTek instruments). ATP hydrolysis was quantified according to the phosphate standard curve prepared by using dipotassium phosphate.

Biochemical Methods. UV−visible spectroscopy for *Sc*Dph4 and *At*Dph4 proteins was carried out on the Cary 5000 UV−vis NIR spectrophotometer (Agilent Technologies), and EPR studies were performed on Biospin (Bruker EPR), Model A200, at 9.42 GHz in the quartz tube under standard conditions as described previously.[31] Energy-dispersive X-ray Spectroscopy (EDS) was done for estimating the elemental composition of proteins by Scanning Electron Microscopy (Zeiss microscope), Ultraplus.[48,49,73]

RESULTS

Omnipresent Nature of Dph4 Proteins. Dph4 is involved in the first step of the DPH biosynthetic pathway in *Saccharomyces cerevisiae*.[19] To better understand the conservation and functionality of the Dph4 protein, we

https://doi.org/10.1021/acsomega.4c01776
ACS Omega 2024, 9, 37650−37661

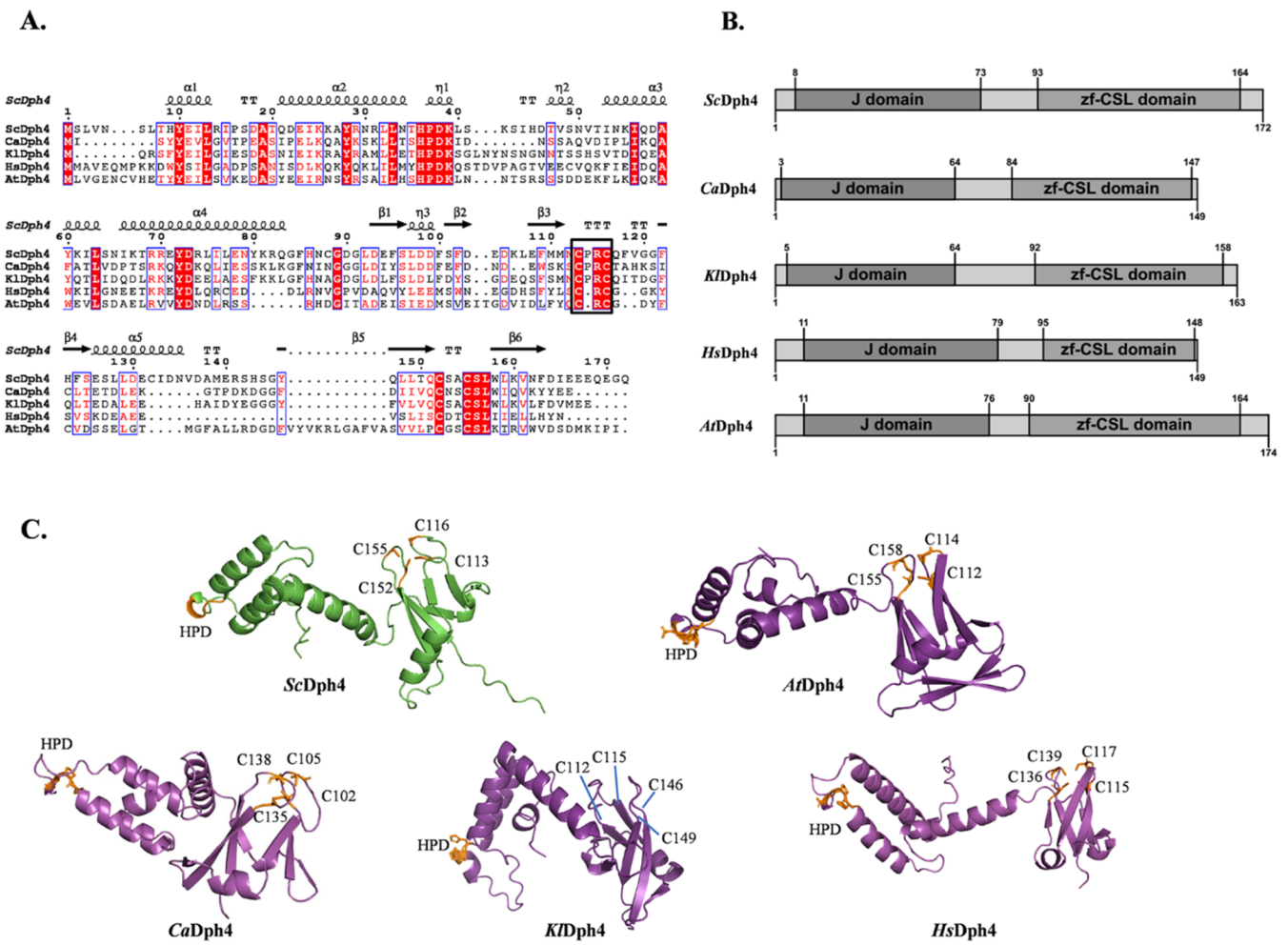

Figure 2. Multiple sequence alignment (MSA) and structural comparison of Dph4 proteins. (A) Five representative Dph4 protein sequences from *S. cerevisiae* *Sc*Dph4, *C. albicans* *Ca*Dph4, *K. lactis* *Kl*Dph4, *H. sapiens* *Hs*Dph4, and *A. thaliana* *At*Dph4 were aligned using MAFFT, and the alignment of the secondary structure was done using ESpript3. Identical residues are highlighted in red, and similar residues are shown in boxes. (B) Domain organization of Dph4 protein. The domains were predicted using the NCBI conserved domain database (CDD), and the structure was made using the IBS tool (Illustrator of biological sequences) (C) Structure of Dph4 protein. The structure comprises a N-terminal J-domain characterized by four α-helices and a C-terminal zF-CSL motif consisting of a three-stranded β-sandwich with one sheet comprising two parallel strands and one antiparallel strand. The second sheet in the β-sandwich is composed of strands running antiparallel to each other. The two β-sheets are separated by a short stretch α-helix. The N-terminal and C-terminal are connected through a linker region (α-helix). The Dph4 protein structure is predicted using α fold 2 tool.

identified orthologs of this protein in different organisms including *Candida albicans*, *Kluyveromyces lactis*, *Homo sapiens*, *and A. thaliana*. Dph4 protein orthologues were found in most but not all of the organisms (Table S2). The multiple sequence alignment of identified orthologs indicates high sequence similarity among them (Figure 2A). The identified orthologues possess the characteristic J-domain at the N-terminus along with the conserved HPD motif and a C-terminal CSL zinc finger motif containing four conserved cysteine residues (Figure 2B). As expected, the predicted structural organization of *Sc*Dph4, *Ca*Dph4, *Kl*Dph4, and *At*Dph4 were similar to the reported structure of Human Dph4 protein[31] (Figure 2C).

Dph4 Function is Highly Conserved across the Species. To test if the function of Dph4 is evolutionarily conserved across the organisms, including plants, we performed a yeast complementation experiment where the *dph4* yeast knockout strain was tested for sensitivity to DT in the presence of Dph4 orthologues from various organisms. Full-length ORFs of these orthologues were cloned in a yeast expression vector under the *TEF1* promoter for moderate overexpression. These constructs carrying different Dph4 orthologues were transformed into *a dph4*Δ strain harboring the catalytic A-chain subunit of DT (*dph4*Δ+DT) under the conditional regulation of the galactose inducible promoter. As expected, the yeast strain lacking Dph4 was resistant to DT on the galactose-containing medium. On the contrary, *dph4*Δ, when complemented with yeast *Sc*Dph4 (wild-type) and, with all of the orthologs, were DT sensitive and dead on the same media (Figure 3A), indicating that heterologous expression of different Dph4 orthologs can substitute for *Sc*Dph4 and can reconstitute the DPH biosynthesis pathway in yeast.

While DPH biosynthesis genes have been studied in *S. cerevisiae*, *Schizosaccharomyces pombe*, *Mus musculus, and H. sapiens*,[10,18−21,50] relatively little is known about them in plants. Only recently, in *Arabidopsis*, the Dph1 protein was identified and reported to be involved in the first step of DPH biosynthesis, which is known to regulate protein synthesis and plant growth.[51] In addition to the highly conserved J-

https://doi.org/10.1021/acsomega.4c01776
ACS Omega 2024, 9, 37650−37661

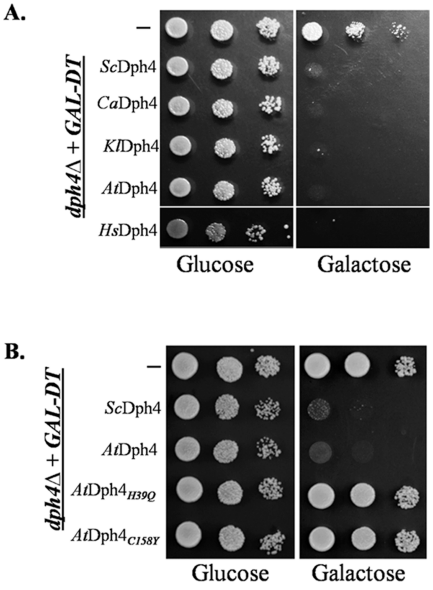

Figure 3. Dph4 protein is functionally conserved across organisms. (A) Five μL of 10-fold serial dilutions of *dph4*Δ cells harboring *GAL-DT* (*dph4*Δ*GAL-DT*) along with an empty pRS413 plasmid empty plasmid (−) or JDP expressing constructs containing Dph4 orthologs from *S. cerevisiae* (*Sc*Dph4), *C. albicans* (*Ca*Dph4), *K. lactis* (*Kl*Dph4), *H. sapiens* (*Hs*Dph4), *A. thaliana* (*At*Dph4) and driven under *TEF* promoter were spotted on Histidine drop-out plates and incubated at 23 °C for 3 days. (B) C-term zf-CSL motif-dependent function of *At*Dph4. Five μL of 10-fold serial dilutions of *dph4*Δ cells harboring *GAL-DT* (*dph4*Δ*GAL-DT*) along with an empty pRS413 plasmid empty plasmid (−) or JDP expressing constructs; pRS413-*TEF-Sc*Dph4 (*Sc*Dph4), pRS413-*TEF-At*Dph4(*At*Dph4), pRS413-*TEF-At*Dph4$_{H39Q}$ (*At*Dph4$_{H39Q}$), and pRS413-*TEF*-atDjC13$_{C158Y}$ (*At*Dph4 $_{C158Y}$) were spotted on His drop-out plates and incubated at 30 °C for 3 days.

domain, Dph4 orthologs also have a conserved zinc finger CSL motif (zf-CSL) at their C-terminus, which is shown to be important for its function in DPH biosynthesis.[31,52] We investigated whether the zf-CSL of *Arabidopsis* Dph4 is required for its function. A "C158A" mutation was created in the C-terminal zf-CSL motif. A plasmid carrying this mutation was transformed into *dph4*Δ+DT. This mutation rendered the protein inactive, and as a result, the cells carrying these mutated genes survived on galactose medium in the presence of DT (Figure 3B). This was similar to the mutation in the J-domain (*At*Dph4$_{H39Q}$), which was shown previously to be inactive for carrying out DPH biosynthesis in budding yeast.[33]

J-domain proteins are known to enhance the ATPase activity of Hsp70s, promoting effective interactions with client proteins and thereby facilitating Hsp70-mediated protein folding and supporting various cellular processes. To determine whether *At*Dph4 retains this capability, Hsp70 ATPase assays were performed. The ability of wild-type (*At*Dph4) and J-domain mutant (*At*Dph4$_{H39Q}$) proteins to stimulate the basal ATPase activity of cytosolic *At*Hsp70-1 (AT5G02500), in the presence of the cytosolic nucleotide exchange factor AtHsp70-14 (AT1G79930), was monitored. *At*Dph4 stimulated the ATPase activity of *At*Hsp70-1 by ∼1.5 fold, while *At*Dph4$_{H39Q}$ could not (Figure S3). This suggests that *At*Dph4 may function as a Hsp70 cochaperone in carrying out DPH biosynthesis in *Arabidopsis*.

***At*Dph4 has Fe-Binding Activity.** The CSL-class zinc-binding family of proteins is known to possess metal-binding capacity due to the presence of negatively charged residues in sequence, including four conserved cysteine residues, with the last cysteine followed by a serine and a leucine residue, forming a metal-binding knuckle.[52] The NMR solution structure of the human Dph4 ortholog has been solved and has been shown to have electron carrier activity, which was attributed to its iron-binding property.[31] This prompted us to investigate whether *At*Dph4 also possessed similar metal-binding properties and compare it with *Sc*Dph4. *Sc*Dph4 and *At*Dph4 were expressed and purified from *E. coli* using His-tag affinity chromatography. A striking difference in color between these two proteins was observed after elution. At equal concentrations (Figure 4A), *At*Dph4 was brown in color, while *Sc*Dph4 was colorless under the same conditions (Figure 4B). We corroborate this observation with an earlier report by Dong et al., where they compared the brown-colored *Sc*Dph3, another zf-CSL motif-containing protein, involved in the DPH biosynthesis pathway, to the colorless *Sc*Dph4 protein.[32]

Metal-binding proteins, including Dph3, TFIIS, and rubredoxin, have been shown to exhibit unique UV−vis spectral profiles with peaks at 350 and 490 nm and a shoulder peak at 570 nm,[32,53] typical characteristic of iron-binding proteins. So, we used UV−visible spectrophotometry to thoroughly characterize the metal-binding property of the *At*Dph4 protein. The UV−vis spectrum for *At*Dph4 also showed a similar UV−vis profile, with peaks at 350, 490, and 570 nm suggesting *At*Dph4 might have some metal affinity. On the other hand, *Sc*Dph4, which was colorless, did not show any of these peaks (Figure 4C). While such UV−vis spectrophotometry indicates iron binding, it does not directly specify the qualitative iron-binding properties of the proteins under investigation.[54] Methods such as electron paramagnetic resonance (EPR) spectroscopy and scanning electron microscopy with energy-dispersive X-ray spectroscopy (SEM-EDS) are the approaches to determine the elemental composition of metal-containing compounds or proteins.[40−42] In principle, SEM exhibits the compositional contrast that results from different atomic number elements and their distribution, while EDS analysis involves the generation of an X-ray spectrum from the entire scan area of the SEM. To show that *At*Dph4 actually binds iron, we subjected the *Sc*Dph4 and *At*Dph4 proteins to EDS function on the SEM and observed the presence of iron. As indicated in the SEM-EDS spectra (Figure 4D), traces of iron were detected in the *At*Dph4 protein, but not in *Sc*Dph4, further confirming that *At*Dph4 has an affinity for iron.

In biological systems, iron can be present in either a ferrous (Fe^{2+}) or ferric (Fe^{3+}) state, depending upon the transition of electrons in the d-subshell orbits. We utilized this property of iron to detect its presence in protein preparations by employing EPR spectroscopy. The detection of iron by EPR spectroscopy depends in principle on the presence of an odd number of electrons, resulting in at least one unpaired electron. This creates an energy difference between the two possible spin states of an electron when an external magnetic field is applied.[55] The EPR spectrum of *At*Dph4 showed resonance at a g value of 4.3, confirming the ferric state, but the same observation was not evident for *Sc*Dph4. This further validates that *At*Dph4 indeed binds to iron (Figure 4E). Put together, we conclude that although functionally similar in the budding

https://doi.org/10.1021/acsomega.4c01776
ACS Omega 2024, 9, 37650−37661

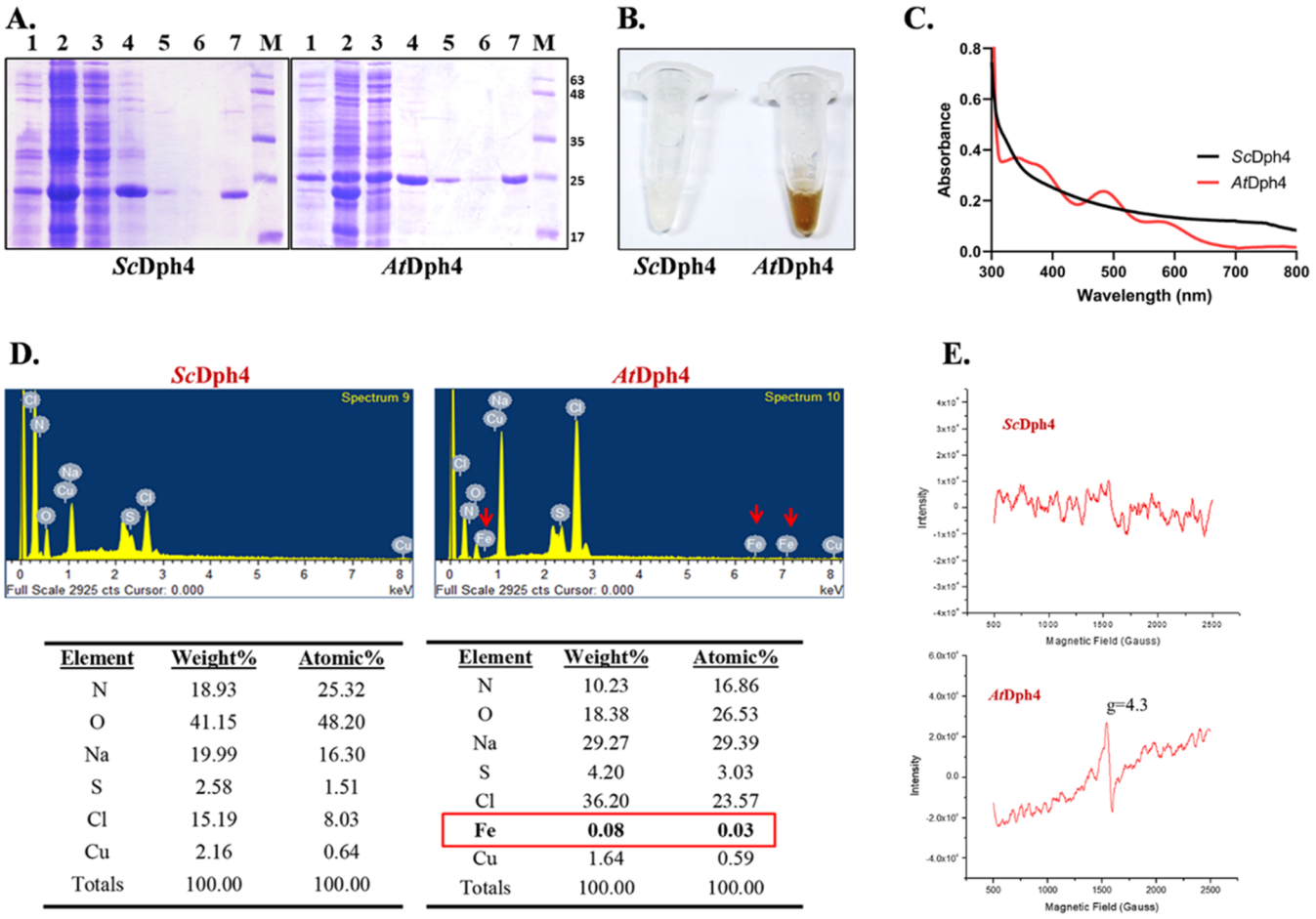

Element	Weight%	Atomic%
N	18.93	25.32
O	41.15	48.20
Na	19.99	16.30
S	2.58	1.51
Cl	15.19	8.03
Cu	2.16	0.64
Totals	100.00	100.00

Element	Weight%	Atomic%
N	10.23	16.86
O	18.38	26.53
Na	29.27	29.39
S	4.20	3.03
Cl	36.20	23.57
Fe	**0.08**	**0.03**
Cu	1.64	0.59
Totals	100.00	100.00

Figure 4. *At*Dph4 has Fe-binding ability. (A−B) *Sc*Dph4 and *At*Dph4 protein expression profile. (A) Coomassie blue-stained SDS-PAGE for protein purification showing profiles for *Sc*Dph4 and *At*Dph4. Lanes 1−7 indicate loading of different sample fractions at various steps, *viz*. 1 whole cell extract, 2 supernatant, 3 pellet, 4 bead-bound protein, 5 bead after elution, 6 flow-through, 7 eluted proteins; M marker. (B) Preparations of *Sc*Dph4 protein (Left) and *Arabidopsis At*Dph4 (Right) purified from *E. coli* Rosetta strain. (C) UV−visible absorption spectra of *Sc*Dph4 (red) and *At*Dph4 (blue) are plotted against wavelength. The peaks at 350 and 490 nm are marked by the arrow symbol. (D) SEM-EDS analysis of *Sc*Dph4 and *At*Dph4. Backscattered electron images in the SEM display compositional contrast that results from different atomic number elements and their distribution. (E) EPR spectra of *Sc*Dph4 and *At*Dph4. Comparison of EPR spectra of *Sc*Dph4 with *At*Dph4 protein preparation recorded at −195.79 °C. The observed resonance of the *At*Dph4 protein is marked for its *g* values.

yeast model, the *Arabidopsis* Dph4 protein has a metal-binding ability in contrast to its yeast counterpart.

Sequence Diversity in the C-Terminal Region Defines the Iron-Binding Property of Dph4 Orthologs. Our UV−visible spectrophotometry and SEM-EDS spectral analysis showed a difference between *At*Dph4 and *Sc*Dph4. To understand the underlying reasons for this difference in iron-binding properties, we undertook a rigorous sequence analysis and homology modeling of Dph4 homologues. Sequence comparison of the Dph4 proteins from different organisms revealed the presence of proline (P) between the first two cysteine residues that form the first loop of the metal-binding knuckle (Figure 5A) in some yeast strains, viz., CPRC in *Sc*Dph4, compared to CRC in *At*Dph4, and the *Hs*Dph4 sequence. This suggests that the presence of two amino acids in budding yeast as compared to one in human and *Arabidopsis* proteins could have an impact on its loop length and thereby on iron binding. This was substantiated by a structural overlap of this part of the proteins, indicating that an extra proline residue between Cys113 and Cys116 causes an increase in the overall length of the loop of Dph4 proteins in yeast species, which might influence their metal-binding abilities (Figure 5B). Since Dph3 and Dph4 share the CSL zinc finger motif, we then compared the sequence of *At*Dph4 with *Sc*Dph3, which is reported to possess iron-binding ability.[32] Interestingly, the CSL motif of *At*Dph4 was found to be 42.31% similar to the CSL motif of *Sc*Dph3, but only 24.24% similar to *Sc*Dph4's CSL motif. According to the NCBI BlastP pairwise alignment, there is no significant similarity between *At*Dph4 and *Sc*Dph4 in the CSL motif. Furthermore, Dph3 proteins have a single proline residue in between the two cysteines, strengthening our loop length hypothesis that sequences with a single amino acid in between the two cysteines, and thus reduced loop length, may coordinate bind iron better than those with more than one amino acid. This is consistent with our data that *At*Dph4, like *Hs*Dph4 and *Sc*Dph3, binds to iron and is thus colored, while *Sc*Dph4 is colorless.

We set out to determine if the proline residue is specifically required for the *Sc*Dph4 functionality or if it is just contributing to the overall loop length, which is crucial for the *Sc*Dph4 function. We first created *Sc*Dph4 constructs where the proline residue was either replaced with an alanine or deleted and tested their functionality in the *dph4*Δ+DT strain. Our results show that the P114A substitution did not

https://doi.org/10.1021/acsomega.4c01776
ACS Omega 2024, 9, 37650−37661

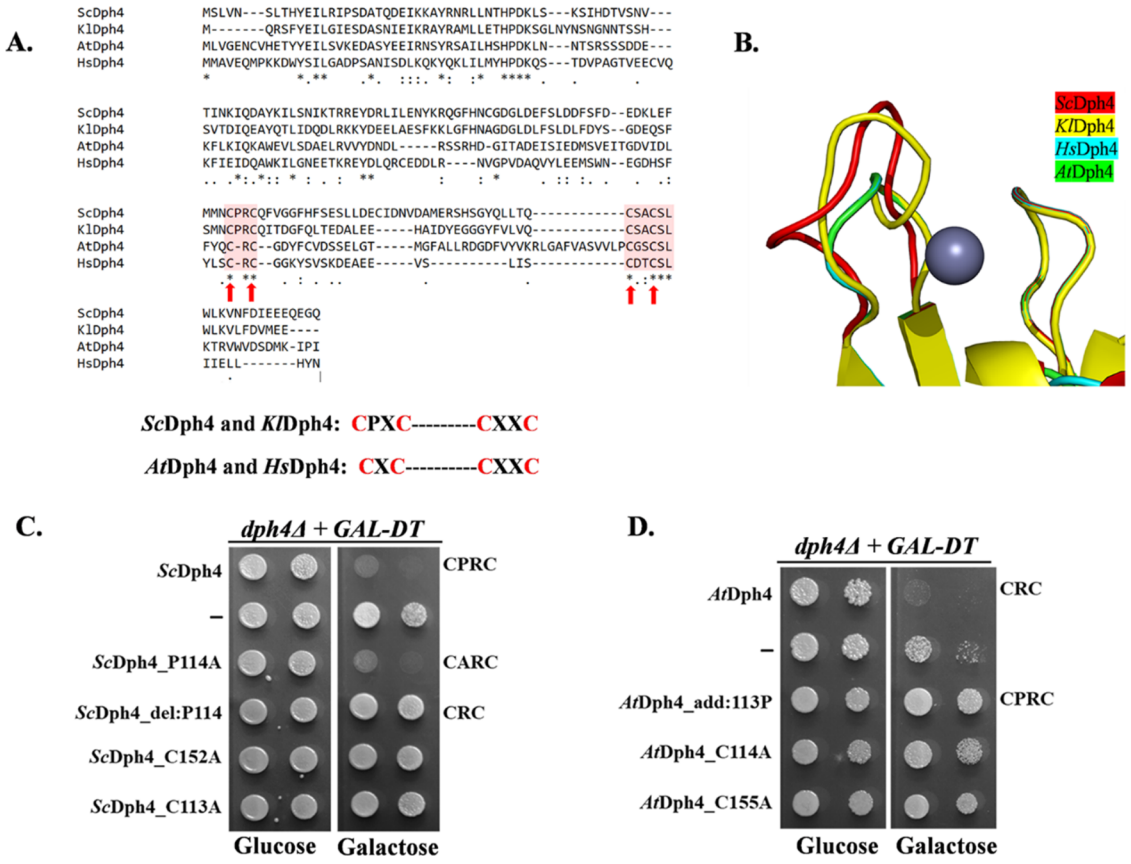

Figure 5. Sequence and structural diversity in the Dph4 CSL motif. (A) Multiple sequence alignment of *Arabidopsis* yeast and human Dph4 orthologs, highlighting the differences in the iron-binding residues. (B) Secondary structure alignment of Dph4 orthologs to highlight the variation in loop length. (C) Five μL of 10-fold serial dilutions of *dph4*Δ cells harboring *GAL-DT* (*dph4 GAL-DT*) along with an empty pRS413 plasmid empty plasmid (−) or Dph4 protein expressing constructs; pRS413-*TEF-Sc*Dph4 (*Sc*Dph4), pRS413-*TEF-Sc*Dph4_P114A (*Sc*Dph4_P114A), pRS413-*TEF-Sc*Dph4_del P114 (*Sc*Dph4_del P114), pRS413-*TEF-At*Dph4_C152A (*At*Dph4_C152A), pRS413-*TEF-At*Dph4_C113A (*At*Dph4_C113A), pRS413-*TEF-At*Dph4 (*At*Dph4), pRS413-*TEF-At*Dph4_C114A (*At*Dph4_C114A), and pRS413-*TEF-At*Dph4_C155A (*At*Dph4_C155A) were spotted on His drop-out plates and incubated at 30 °C for 3 days.

affect the functionality of *Sc*Dph4, as *dph4*Δ+DT cells harboring P114A mutations carrying *Sc*Dph4 plasmids were unable to grow on galactose-containing plates (Figure 5C). In contrast, proline deletion completely abrogated *Sc*Dph4 function, as the cells survived on the galactose-containing medium. Next, we tested the importance of loop length in the *Arabidopsis* Dph4 protein. For this, we created an *At*Dph4 construct where a proline was inserted between the cysteine residues (P114), forming the metal-binding loop, and tested its functionality in the *dph4*Δ+DT strain. Interestingly, the presence of this extra proline renders *At*Dph4 inactive in budding yeast as it failed to complement the *dph4*Δ+DT strain (Figure 5D).

Next, we investigated the functional relevance of the conserved cysteines in the zf-CSL motif of *Sc*Dph4 and *At*Dph4. For this, cysteine 113 and 152 from *Sc*Dph4 and cysteine 114 and 155 from *At*Dph4 were chosen and replaced with alanine using site-directed mutagenesis. These mutation-carrying constructs were tested for their ability to complement the Dph4 deficiency in the *dph4*Δ+DT strain. As expected, these alanine substitutions evade both the *Sc*Dph4 and *At*Dph4 functions as they failed to rescue the *dph4*Δ+DT strain on galactose-containing medium (Figure 5D), signifying the highly conserved nature of cysteine residues in the formation of a metal-binding loop proving the essentiality of cysteine residues in both *Sc*Dph4 and *At*Dph4 function.

To test the expression of *At*Dph4 mutants, all of the constructs were transformed into the *dph4*Δ strain. The total protein lysate of the yeast transformants was analyzed by Western using the *At*Dph4 antibodies. While the wild-type (*At*Dph4) and J-domain mutant ($AtDph4_{H39Q}$) proteins were expressed at comparable levels, most other mutants were expressed at lower levels in budding yeast (Figure S1).

To analyze if these proteins were properly folded and if their levels were sufficiently high to perform their role in DPH biosynthesis, we took an indirect approach. All of the constructs expressing *At*Dph4, $AtDph4_{H39Q}$, $AtDph4_{C158Y}$, *At*Dph4_add:113P, *At*Dph4_C114A, and *At*Dph4_C155A were transformed into the *ydj1*Δ strain. We hypothesized that, if properly folded, having a functional J-domain, all of the proteins, except $AtDph4_{H39Q}$, should interact with Hsp70 and rescue the temperature sensitivity of yeast cells lacking Ydj1. Ydj1 is the most abundant J-domain protein in the yeast cytosol. Its deficiency makes yeast cells sick, which can be efficiently rescued by overexpression of J-domains containing proteins.[34] All of the *At*Dph4 variants, except the J-domain mutation, $AtDph4_{H39Q}$, were able to rescue the "slow-growth" phenotype of the Ydj1 deletion strain, signifying their ability to stimulate the weak ATPase activity of cytosolic Hsp70 (Figure S2). These results indicate two things: First, these variants are expressed at sufficiently high levels. Second, these proteins are stable and properly folded *in vivo* and their inability to rescue

https://doi.org/10.1021/acsomega.4c01776
ACS Omega 2024, 9, 37650−37661

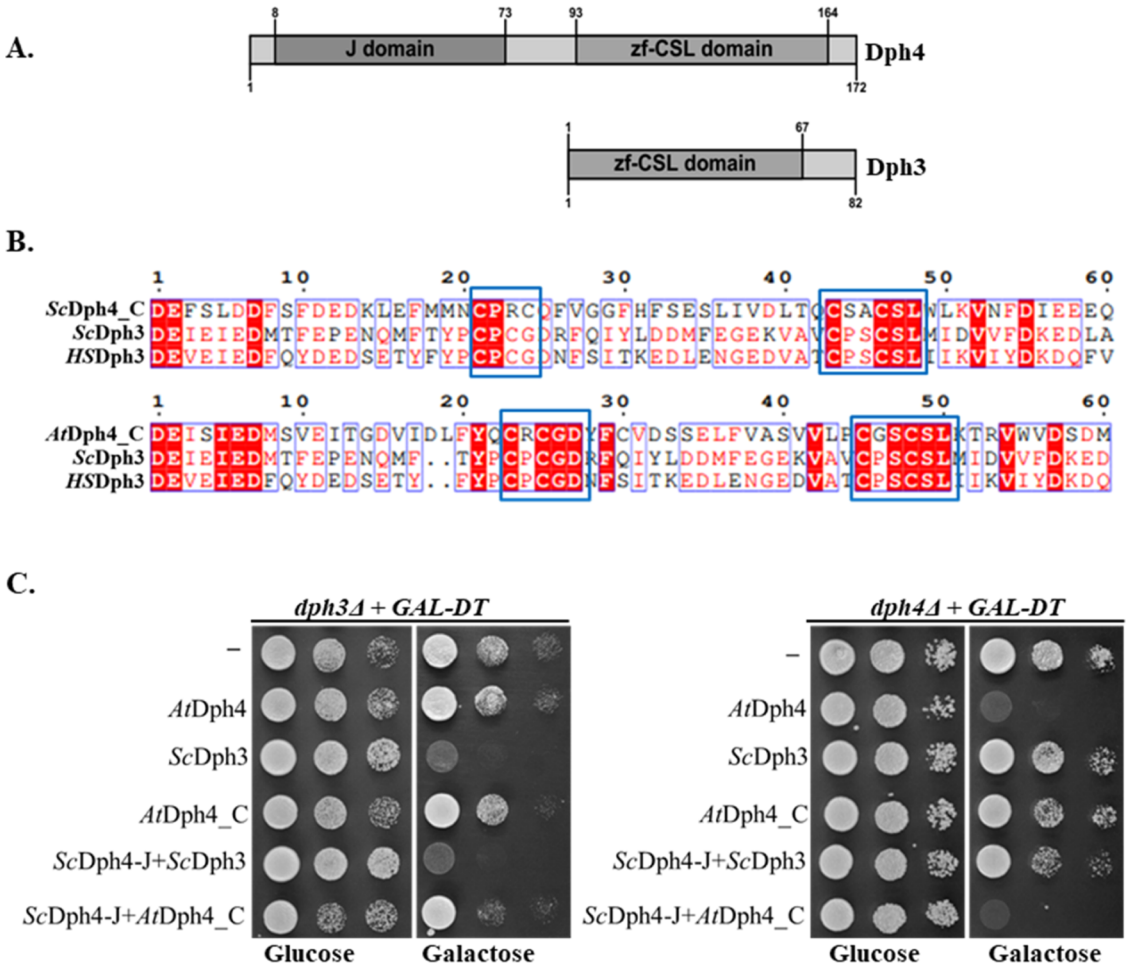

Figure 6. *At*Dph4 and *Sc*Dph3 are structurally similar, though distinct functionally. (A) Dph3 and Dph4 proteins share the zf-CSL motif. The domain organization was predicted using NCBI CDD, and the structural representation was done using the IBS tool. (B) Sequence alignment of the C-terminal zf-CSL motif of Dph4 with the zf-CSL motif of *Sc*Dph3 and *Hs*Dph3 proteins; the alignment was visualized in Espript3. Similar residues are shown in boxes, and identical residues are highlighted in red. (C) Five μL of 10-fold serial dilutions of wild-type cells harboring *GAL-DT* along with an empty pRS413 plasmid (WT-*GAL-DT*) and *dph3*Δ cells either with an empty plasmid (−) or different gene expressing constructs pRS413-*TEF*-*At*Dph4 (*At*Dph4), pRS413-*TEF*-Dph3 (Dph3), pRS413-*TEF*-*At*Dph4-C terminal fragment (*At*Dph4-C), pRS413-*TEF*- chimera construct of J-domain of Dph4 fused with Dph3 (*Sc*Dph4-J+Dph3), and pRS413-*TEF*- chimera construct of J-domain of *Sc*Dph4 fused with *At*Dph4-C terminal (*Sc*Dph4-J+*At*Dph4-C) were spotted on His DO plates containing glucose and galactose and incubated at 30 °C for 3 days.

DPH biosynthesis defect of *dph4*Δ is due to compromised function in yeast cells.

***Sc*Dph3 *and At*Dph4 are Functionally Distinct.** *At*Dph4 shares the conserved zf-CSL motif with the Dph3 protein, which has iron-binding activity and works as a redox-active protein during DPH biosynthesis.[32] Since *At*Dph4 shares common structural elements, sequential features (Figure 6A,B), and also iron-binding ability, we examined if *At*Dph4 could replace Dph3 in *dph3*Δ cells and restore DPH biosynthesis. For this, we transformed the full-length *At*Dph4 construct in *dph3*Δ+DT cells. Our results showed that *At*Dph4 could not complement the DPH biosynthesis defects of Δ*dph3* (Figure 6C). Since the similarity between Dph3 and *At*Dph4 is only in the zf-CSL motif, we reasoned that possibly the presence of a J-domain tethers *At*Dph4 to Hsp70, thereby compromising its ability to substitute for Dph3 in budding yeast. So, we generated an *At*Dph4-C construct encompassing only residues 77-174 of *At*Dph4 lacking the N-terminal J-domain. Like full-length *At*Dph4, expression of C-terminus too could not restore DPH biosynthesis as *dph3*Δ+DT cells expressing the *At*Dph4-C mutant grew like *dph3*Δ [*Gal-DT*] cells with an empty plasmid (Figure 6C). We further tested this idea using an alternative approach. Using the PCR sewing method, we inserted the J-domain fragment of *Sc*Dph4 (residues 1-73) to the N-terminus of Dph3 to make a chimeric construct [*Sc*Dph4-J+*Sc*Dph3], assuming this protein would functionally behave like *At*Dph4. We made another chimera construct [*Sc*Dph4-J+*At*Dph4-C] where the same J-domain fragment was fused with *At*Dph4-C (77-174) as a control. The functionality of these chimeric proteins was tested in both *dph3*Δ+DT and *dph4*+DT cells. The [*Sc*Dph4-J+*Sc*Dph3] chimeric protein rescued *dph3*Δ+DT cells but failed to do so in *dph4*Δ+DT cells; on the other hand, [*Sc*Dph4-J+*At*Dph4-C] rescued the *dph4*Δ+DT cells but failed to complement *dph3*Δ+DT cells. Our results show that even though these two proteins display remarkable structural and biochemical similarity, *At*Dph4 and *Sc*Dph3 are functionally distinct and have very specific and nonredundant requirements in the DPH biosynthesis process.

https://doi.org/10.1021/acsomega.4c01776
ACS Omega 2024, 9, 37650−37661

DISCUSSION

DPH is an archaebacterial and eukaryotic post-translational modification that has been conserved during evolution. Its pathobiological relevance is well established, but its biological significance is still elusive. DPH's presence in domain IV of eEF2 suggests its role in the maintenance of translational fidelity.[16,17] DPH has also been implicated in specific translational regulation under stress; it regulates selenoprotein translation and internal ribosomal entry site (IRES) mediated translation DPH biosynthesis machinery is also highly conserved.[56,57] All Dph1-7 genes have been found conserved in yeast, mice, and humans.[16,17] So far, only two proteins involved in the first step of DPH biosynthesis have been identified in plants, *At*Dph1 and *At*Dph4.[33,51] A recent publication established the existence of DPH in plants and showed that *At*Dph1 (AT5G62030) is essential for translational fidelity; just like the yeast mutants, *dph1* mutants are sensitive to translational inhibitors and have defects in the TOR pathway, thus displaying abnormalities in growth.[33,51] In a previous study, we discovered the *Arabidopsis* ortholog for the Dph4 protein, *At*Dph4 (atDjC13/AT4G10130), and showed that *At*Dph4 can replace Jjj3/*Sc*Dph4 for DPH biosynthesis in budding yeast, suggesting that its function is conserved across species.[33,51]

Dph4 is a bipartite protein with an N-terminal J-domain and a C-terminal CSL zinc finger motif. Dph4's J-domain is required for DPH biosynthesis and also for stimulation of Hsp70 protein ATPase activity.[31,58] The J-domain of *At*Dph4 is known to be required for DPH biosynthesis.[33] Other than being a Hsp70 cochaperone, human Dph4 has roles such as iron binding, redox, and electron carrier activity governed by its C-terminal motif. Human Dph4 binds to both zinc and iron via four conserved cysteine residues in the CSL motif.[31,58] These residues are critical for the function of yeast and human Dph4 genes in DPH biosynthesis.[31,34] Consistent with that, C158Y, C114A, and C155A substitutions in *At*Dph4 rendered the protein nonfunctional, resulting in no DPH synthesis and thus resistance to DT in the yeast cells lacking *Sc*Dph4. Moreover, purified *At*Dph4 could bind iron, as verified by UV−visible and SEM-EDS spectra. This suggests that like *Hs*Dph4 and Dph3, *At*Dph4 could act as an electron donor for Dph1 and Dph2 iron−sulfur clusters.[31,58] Similar to *Hs*Dph4 and other Zn-CSL motif-containing proteins, *At*Dph4 might also coordinate with the zinc metal. However, further experiments are needed to confirm this possibility. Beyond DPH biosynthesis, *At*Dph4 may also have a moonlighting iron-binding/redox function. *At*Dph4 orthologs could be functioning like DJA6 and DJA5, which are *Arabidopsis* type-I J-proteins that bind iron via conserved cysteine residues in the cysteine-rich (CR) domain and enable iron incorporation into Fe−S clusters through their interactions with the sulfur utilization factor (SUF) apparatus via their J-domain.[59] The absence of these two proteins results in severe abnormalities in the accumulation of chloroplast Fe−S proteins, photosynthetic dysfunction, and considerable intracellular iron overload.[59] Another JDP, *At*HSCB, plays an important role in the regulation of the Fe−S assembly pathway in plant mitochondria, thus maintaining iron homeostasis.[60−62] Just like the chloroplast and mitochondrial JDPs, *At*Dph4, being localized to the cytoplasm, might be a component of CIA (cytosolic iron−sulfur protein assembly) machinery and regulate the iron homeostasis in the cytosol. A recent study that examined the impact of iron and sulfate deficiency on levels of DPH modification, discovered that the iron- and sulfate-deficient *Arabidopsis* mutants have slightly increased levels of unmodified eEF2 than wild-type controls.[33,51] DPH modification states are thus dependent on iron and sulfur availability, as four proteins involved in the first step require iron for their function, while Dph1 and 2 contain ISCs, and Dph3 and Dph4 bind iron via CSL motifs. However, whether or not the iron-binding activity of *At*Dph4 is important *in vivo* needs to be further investigated.

Sequence analysis and homology modeling of the metal-binding loop in Dph4 homologues support the idea of an optimum loop length on iron binding. This is further corroborated by the fact that *Hs*Dph4, *At*Dph4 as well as Dph3 proteins, which have shorter metal-binding knuckles bind iron and *Sc*Dph4 does not. Interestingly, the P114A substitution did not affect the functionality of *Sc*Dph4, while its deletion completely abrogated the *Sc*Dph4 function. On the other hand, the presence of extra proline in *At*Dph4 had a deleterious effect on protein function. This indicates that structural changes in this region are not only responsible for unique metal-binding abilities in complex eukaryotes such as plants and humans but also have a greater functional relevance in different organisms.

Despite the remarkable biochemical similarity shared by *At*Dph4 and Dph3, our results from the chimeras do not unequivocally prove an evolutionary relationship between these two proteins. Although they are involved in the same cellular process (DPH biosynthesis), both *At*Dph4 and Dph3 are functionally distinct. We believe that Dph3 is the main protein for all of the redox activities and acts as a reductant in Fe−S cluster assembly during DPH biosynthesis. On the other hand, Dph4 orthologs in more complex eukaryotes, like humans and plants, work as an Hsp70 cochaperone, playing a role in assisting the formation of Fe−S cluster assembly and, at the same time, buffering the electron transfer activity of Dph3; however, this needs to be experimentally validated.

At this point, we cannot rule out the possibility that *At*Dph4 may be involved in functions other than DPH biosynthesis, as well. *Sc*Dph4 is known to interact with protein kinases involved in different processes.[63] Likewise, *At*Dph4 interacts with the mitogen-activated protein kinase 1 (*At*MPK1),[64] which is activated upon wounding, indicating a role of *At*Dph4 in defense response. A recent study reveals that *At*Dph4 plays a role in plant defense against Turnip mosaic potyvirus infection; consequently, *At*Dph4 loss of function mutants displayed significantly enhanced disease progression in comparison to WT plants.[65] *Hs*Dph4 is regulated via HSF2 transcriptional regulation under extracellular stress conditions.[66] The methylation of DPH4 promoters influences diphthamide synthesis and toxin sensitivity in tumor cells, demonstrating that DPH gene expression impacts diphthamide synthesis.[67] According to *in-silico* expression data at GENEINVESTIGATOR[68] and eEFP browser (http://bar.utoronto.ca/efp2/Arabidopsis/Arabidopsis_eFPBrowser2.html).[69] *At*Dph4 is expressed in almost all stages of growth and development as well as under a variety of biotic and abiotic conditions. Interestingly, an ARE element-AAACCA, which is required for anaerobic induction, was also found in the *At*Dph4 promoter. Anaerobic conditions are required for ISC assembly.[66,70] Thus, *At*Dph4 like *Hs*Dph4 may have a role in growth and development as well as the biotic or abiotic stress response.

https://doi.org/10.1021/acsomega.4c01776
ACS Omega 2024, 9, 37650−37661

The Dph4 homologues in complex eukaryotes like plants and humans exhibit metal-binding capabilities. Such a kind of novel gains of functions has been reported in other JDPs as well. For example, Cwc23, a type III JDP possesses an additional C-terminal RNA Recognition motif (RRM) in its *Arabidopsis* and human ortholog that imparts these proteins a unique RNA binding ability, which is absent in the *S. cerevisiae* ortholog, *Sc*Cwc23.[71] Considering that fungi and animals are monophyletic and plants diverged much earlier, the most parsimonious interpretation is that the iron-binding property was possibly lost in the common ancestor of Saccharomycetaceae. Such events of neofunctionalization could be instrumental in generating evolutionary novelty with a greater adaptability to more complex environments.

CONCLUSIONS

In conclusion, our research work highlights the significance of the C-terminal domain of type III JDP, *At*Dph4 and reveals its novel iron-binding abilities. As genes involved in the DPH biosynthesis pathway are characterized in different systems, including plants, the importance of this unusual, yet conserved post-translational modification in growth and development is coming to light. It remains to be seen if the ability of *At*Dph4 to bind iron is important in either DPH biosynthesis or in a yet unknown cellular process requiring redox activity. Nevertheless, this study presents an example of how structural modifications in JDPs are responsible for imparting unique combinations of functions in complex eukaryotes, enabling adaptation to complex environments.

ASSOCIATED CONTENT

Supporting Information

The Supporting Information is available free of charge at https://pubs.acs.org/doi/10.1021/acsomega.4c01776.

Table S1. List of primers used in this study. Table S2: List of Dph4 orthologs found in different species. Figure S1: Expressions of *At*Dph4 mutants. Figure S2: *At*Dph4 mutants rescue the *ydj1*Δstrain. Figure S3: *At*Dph4 stimulates ATPase activity of *At*Hsp70-1 (PDF)

Accession Codes

Arabidopsis thaliana Dph4 (O82623), *Homo sapiens* Dph4 (Q6P3W2), *Saccharomyces cerevisiae* Dph4 (P47138), *and Saccharomyces cerevisiae* Dph3 (Q3E840).

AUTHOR INFORMATION

Corresponding Authors

Zeyaul Islam − *Department of Biological Sciences, Indian Institute of Science Education and Research, Bhopal, Madhya Pradesh 462066, India; Diabetes Research Center (DRC), Qatar Biomedical Research Institute (QBRI), Hamad Bin Khalifa University (HBKU), Qatar Foundation, 34110 Doha, Qatar;* orcid.org/0000-0002-5444-3910; Email: zislam@hbku.edu.qa

Chandan Sahi − *Department of Biological Sciences, Indian Institute of Science Education and Research, Bhopal, Madhya Pradesh 462066, India;* orcid.org/0000-0002-4821-9736; Email: sahi@iiserb.ac.in

Authors

Amit Kumar Verma − *Department of Biological Sciences, Indian Institute of Science Education and Research, Bhopal, Madhya Pradesh 462066, India; Department of Internal Medicine, UT Southwestern Medical Center, Dallas, Texas 75390-9096, United States;* orcid.org/0000-0003-4928-8458

Priya Sharma − *Department of Botany, Faculty of Science, University of Delhi, Delhi 110007, India;* orcid.org/0000-0001-8353-8057

Anup Kumar Biswal − *Department of Biological Sciences, Indian Institute of Science Education and Research, Bhopal, Madhya Pradesh 462066, India*

Yogesh Tak − *Center for Alzheimer's and Neurodegenerative Diseases, Peter O'Donnell Jr. Brian Institute, UT Southwestern Medical Center, Dallas, Texas 75390-9096, United States*

Complete contact information is available at: https://pubs.acs.org/10.1021/acsomega.4c01776

Author Contributions

#A.K.V. and P.S. contributed equally. C.S., Z.I., and A.K.V. conceptualized and planned the experiment. A.K.V., Z.I., A.K.B., Y.T., and P.S. carried out the experiments. A.K.V., Z.I., and P.S. performed the *in-silico* analysis. A.K.V., P.S., and C.S. analyzed the results and wrote the manuscript.

Funding

A.K.V. thanks GATE fellowship, MHRD, India; P.S. and A.K.B. thank CSIR, New Delhi, for fellowship. This work was supported by funds from the Department of Biotechnology (DBT/PR6885/GBD/27/488/2012), the Department of Science and Technology (EMR/2015/001213), RGYI (SAN No.102/IFD/SAN/2131/2013-2014), and intramural funds from IISER Bhopal to C.S.

Notes

The authors declare no competing financial interest.

ACKNOWLEDGMENTS

We thank Elizabeth Craig (UW-Madison, USA) for donating yeast strains and plasmids. We thank IISER Bhopal's Central instrumentation facility for providing SEM, EPR, and UV−vis facilities.

ABBREVIATIONS

JDPs, J-domain proteins; Hsp70, heat shock protein 70; DPH, diphthamide; DT, diphtheria toxin; Fe-Dph4, iron-bound Dph4; Zn-Dph4, zinc-bound Dph4; PTMs, post-translational modifications; EF2, elongation factor 2

REFERENCES

(1) Walsh, P.; Bursać, D.; Law, Y. C.; Cyr, D.; Lithgow, T. The J-protein Family: Modulating Protein Assembly, Disassembly and Translocation. *EMBO Rep.* **2004**, *5* (6), 567−571.

(2) Seet, B. T.; Dikic, I.; Zhou, M.-M.; Pawson, T. Reading Protein Modifications with Interaction Domains. *Nat. Rev. Mol. Cell Biol.* **2006**, *7* (7), 473−483.

(3) Ramazi, S.; Zahiri, J. Post-Translational Modifications in Proteins: Resources, Tools and Prediction Methods. *Database* 2021, *2021*. DOI: 10.1093/database/baab012.

(4) Yang, X.-J. Multisite Protein Modification and Intramolecular Signaling. *Oncogene* **2005**, *24* (10), 1653−1662.

(5) Robinson, E. A.; Henriksen, O.; Maxwell, E. S. Elongation Factor 2. *J. Biol. Chem.* **1974**, *249* (16), 5088−5093.

(6) Van Ness, B. G.; Howard, J. B.; Bodley, J. W. ADP-Ribosylation of Elongation Factor 2 by Diphtheria Toxin. Isolation and Properties of the Novel Ribosyl-Amino Acid and Its Hydrolysis Products. *J. Biol. Chem.* **1980**, *255* (22), 10717−10720.

(7) Kimata, Y.; Kohno, K. Elongation Factor 2 Mutants Deficient in Diphthamide Formation Show Temperature-Sensitive Cell Growth. *J. Biol. Chem.* **1994**, *269* (18), 13497−13501.
(8) Ortiz, P. A.; Ulloque, R.; Kihara, G. K.; Zheng, H.; Kinzy, T. G. Translation Elongation Factor 2 Anticodon Mimicry Domain Mutants Affect Fidelity and Diphtheria Toxin Resistance. *J. Biol. Chem.* **2006**, *281* (43), 32639−32648.
(9) Bär, C.; Zabel, R.; Liu, S.; Stark, M. J. R.; Schaffrath, R. A Versatile Partner of Eukaryotic Protein Complexes That Is Involved in Multiple Biological Processes: Kti11/Dph3. *Mol. Microbiol.* **2008**, *69* (5), 1221−1233.
(10) Liu, S.; Bachran, C.; Gupta, P.; Miller-Randolph, S.; Wang, H.; Crown, D.; Zhang, Y.; Wein, A. N.; Singh, R.; Fattah, R.; Leppla, S. H. Diphthamide Modification on Eukaryotic Elongation Factor 2 Is Needed to Assure Fidelity of mRNA Translation and Mouse Development. *Proc. Natl. Acad. Sci. U.S.A.* **2012**, *109* (34), 13817−13822.
(11) Uthman, S.; Bär, C.; Scheidt, V.; Liu, S.; ten Have, S.; Giorgini, F.; Stark, M. J. R.; Schaffrath, R. The Amidation Step of Diphthamide Biosynthesis in Yeast Requires DPH6, a Gene Identified through Mining the DPH1-DPH5 Interaction Network. *PLoS Genet.* **2013**, *9* (2), No. e1003334.
(12) Collier, R. J. Diphtheria Toxin: Mode of Action and Structure. *Bacteriol. Rev.* **1975**, *39* (1), 54−85.
(13) Iglewski, B. H.; Liu, P. V.; Kabat, D. Mechanism of Action of *Pseudomonas Aeruginosa* Exotoxin Aiadenosine Diphosphate-Ribosylation of Mammalian Elongation Factor 2 in Vitro and in Vivo. *Infect. Immun.* **1977**, *15* (1), 138−144.
(14) Wilson, B. A.; Collier, R. J. Diphtheria Toxin and *Pseudomonas Aeruginosa* Exotoxin A: Active-Site Structure and Enzymic Mechanism. *Curr. Top. Microbiol. Immunol.* **1992**, *175*, 27−41.
(15) Jørgensen, R.; Purdy, A. E.; Fieldhouse, R. J.; Kimber, M. S.; Bartlett, D. H.; Merrill, A. R. Cholix Toxin, a Novel ADP-Ribosylating Factor from *Vibrio Cholerae*. *J. Biol. Chem.* **2008**, *283* (16), 10671−10678.
(16) Schaffrath, R.; Abdel-Fattah, W.; Klassen, R.; Stark, M. J. R. The Diphthamide Modification Pathway from *Saccharomyces Cerevisiae* − Revisited. *Mol. Microbiol.* **2014**, *94* (6), 1213−1226.
(17) Tsuda-Sakurai, K.; Miura, M. The Hidden Nature of Protein Translational Control by Diphthamide: The Secrets under the Leather. *J. Biochem.* **2019**, *165* (1), 1−8.
(18) Chen, J. Y.; Bodley, J. W.; Livingston, D. M. Diphtheria Toxin-Resistant Mutants of *Saccharomyces Cerevisiae*. *Mol. Cell. Biol.* **1985**, *5* (12), 3357−3360.
(19) Liu, S.; Milne, G. T.; Kuremsky, J. G.; Fink, G. R.; Leppla, S. H. Identification of the Proteins Required for Biosynthesis of Diphthamide, the Target of Bacterial ADP-Ribosylating Toxins on Translation Elongation Factor 2. *Mol. Cell. Biol.* **2004**, *24* (21), 9487−9497.
(20) Webb, T. R.; Cross, S. H.; McKie, L.; Edgar, R.; Vizor, L.; Harrison, J.; Peters, J.; Jackson, I. J. Diphthamide Modification of eEF2 Requires a J-Domain Protein and Is Essential for Normal Development. *J. Cell Sci.* **2008**, *121* (19), 3140−3145.
(21) Stahl, S.; da Silva Mateus Seidl, A. R.; Ducret, A.; Kux van Geijtenbeek, S.; Michel, S.; Racek, T.; Birzele, F.; Haas, A. K.; Rueger, R.; Gerg, M.; Niederfellner, G.; Pastan, I.; Brinkmann, U. Loss of Diphthamide Pre-Activates NF-κB and Death Receptor Pathways and Renders MCF7 Cells Hypersensitive to Tumor Necrosis Factor. *Proc. Natl. Acad. Sci. U.S.A.* **2015**, *112* (34), 10732−10737.
(22) Cinà, D. P.; Ketela, T.; Brown, K. R.; Chandrashekhar, M.; Mero, P.; Li, C.; Onay, T.; Fu, Y.; Han, Z.; Saleem, M.; Moffat, J.; Quaggin, S. E. Forward Genetic Screen in Human Podocytes Identifies Diphthamide Biosynthesis Genes as Regulators of Adhesion. *Am. J. Physiol.: Renal Physiol.* **2019**, *317* (6), F1593−F1604.
(23) Gillies, A. T.; Taylor, R.; Gestwicki, J. E. Synthetic Lethal Interactions in Yeast Reveal Functional Roles of J Protein Co-Chaperones. *Mol. BioSyst.* **2012**, *8* (11), 2901.
(24) Zhang, Y.; Lin, Z.; Zhu, J.; Wang, M.; Lin, H. Diphthamide Promotes TOR Signaling by Increasing the Translation of Proteins in the TORC1 Pathway. *Proc. Natl. Acad. Sci. U.S.A.* **2021**, *118* (37), No. e2104577118, DOI: 10.1073/pnas.2104577118.
(25) Hawer, H.; Ütkür, K.; Arend, M.; Mayer, K.; Adrian, L.; Brinkmann, U.; Schaffrath, R. Importance of Diphthamide Modified EF2 for Translational Accuracy and Competitive Cell Growth in Yeast. *PLoS One* **2018**, *13* (10), No. e0205870.
(26) Kampinga, H. H.; Andreasson, C.; Barducci, A.; Cheetham, M. E.; Cyr, D.; Emanuelsson, C.; Genevaux, P.; Gestwicki, J. E.; Goloubinoff, P.; Huerta-Cepas, J.; Kirstein, J.; Liberek, K.; Mayer, M. P.; Nagata, K.; Nillegoda, N. B.; Pulido, P.; Ramos, C.; De los Rios, P.; Rospert, S.; Rosenzweig, R.; Sahi, C.; Taipale, M.; Tomiczek, B.; Ushioda, R.; Young, J. C.; Zimmermann, R.; Zylicz, A.; Zylicz, M.; Craig, E. A.; Marszalek, J. Function, Evolution, and Structure of J-Domain Proteins. *Cell Stress Chaperones* **2019**, *24* (1), 7−15.
(27) Kampinga, H. H.; Craig, E. A. The HSP70 Chaperone Machinery: J Proteins as Drivers of Functional Specificity. *Nat. Rev. Mol. Cell Biol.* **2010**, *11* (8), 579−592.
(28) Verma, A. K.; Tamadaddi, C.; Tak, Y.; Lal, S. S.; Cole, S. J.; Hines, J. K.; Sahi, C. The Expanding World of Plant J-Domain Proteins. *Crit. Rev. Plant Sci.* **2019**, *38* (5−6), 382−400.
(29) Rosenzweig, R.; Nillegoda, N. B.; Mayer, M. P.; Bukau, B. The Hsp70 Chaperone Network. *Nat. Rev. Mol. Cell Biol.* **2019**, *20* (11), 665−680.
(30) Craig, E. A.; Marszalek, J. How Do J-Proteins Get Hsp70 to Do So Many Different Things? *Trends Biochem. Sci.* **2017**, *42* (5), 355−368.
(31) Thakur, A.; Chitoor, B.; Goswami, A. V.; Pareek, G.; Atreya, H. S.; D'Silva, P. Structure and Mechanistic Insights into Novel Iron-Mediated Moonlighting Functions of Human J-Protein Cochaperone, Dph4. *J. Biol. Chem.* **2012**, *287* (16), 13194−13205.
(32) Dong, M.; Su, X.; Dzikovski, B.; Dando, E. E.; Zhu, X.; Du, J.; Freed, J. H.; Lin, H. Dph3 Is an Electron Donor for Dph1-Dph2 in the First Step of Eukaryotic Diphthamide Biosynthesis. *J. Am. Chem. Soc.* **2014**, *136* (5), 1754−1757.
(33) Verma, A. K.; Diwan, D.; Raut, S.; Dobriyal, N.; Brown, R. E.; Gowda, V.; Hines, J. K.; Sahi, C. Evolutionary Conservation and Emerging Functional Diversity of the Cytosolic Hsp70:J Protein Chaperone Network of *Arabidopsis Thaliana*. *G3: Genes, Genomes, Genet.* **2017**, *7* (6), 1941−1954.
(34) Sahi, C.; Craig, E. A. Network of General and Specialty J Protein Chaperones of the Yeast Cytosol. *Proc. Natl. Acad. Sci. U.S.A.* **2007**, *104* (17), 7163−7168.
(35) Boratyn, G. M.; Camacho, C.; Cooper, P. S.; Coulouris, G.; Fong, A.; Ma, N.; Madden, T. L.; Matten, W. T.; McGinnis, S. D.; Merezhuk, Y.; Raytselis, Y.; Sayers, E. W.; Tao, T.; Ye, J.; Zaretskaya, I. BLAST: A More Efficient Report with Usability Improvements. *Nucleic Acids Res.* **2013**, *41* (W1), W29−W33.
(36) Cherry, J. M.; Hong, E. L.; Amundsen, C.; Balakrishnan, R.; Binkley, G.; Chan, E. T.; Christie, K. R.; Costanzo, M. C.; Dwight, S. S.; Engel, S. R.; Fisk, D. G.; Hirschman, J. E.; Hitz, B. C.; Karra, K.; Krieger, C. J.; Miyasato, S. R.; Nash, R. S.; Park, J.; Skrzypek, M. S.; Simison, M.; Weng, S.; Wong, E. D. Saccharomyces Genome Database: The Genomics Resource of Budding Yeast. *Nucleic Acids Res.* **2012**, *40* (D1), D700−D705.
(37) Berardini, T. Z.; Reiser, L.; Li, D.; Mezheritsky, Y.; Muller, R.; Strait, E.; Huala, E. The Arabidopsis Information Resource: Making and Mining the "Gold Standard" Annotated Reference Plant Genome. *Genesis* **2015**, *53* (8), 474−485.
(38) Gabaldón, T.; Koonin, E. V. Functional and Evolutionary Implications of Gene Orthology. *Nat. Rev. Genet.* **2013**, *14* (5), 360−366.
(39) Katoh, K. MAFFT: A Novel Method for Rapid Multiple Sequence Alignment Based on Fast Fourier Transform. *Nucleic Acids Res.* **2002**, *30* (14), 3059−3066.
(40) Robert, X.; Gouet, P. Deciphering Key Features in Protein Structures with the New ENDscript Server. *Nucleic Acids Res.* **2014**, *42* (W1), W320−W324.
(41) Lu, S.; Wang, J.; Chitsaz, F.; Derbyshire, M. K.; Geer, R. C.; Gonzales, N. R.; Gwadz, M.; Hurwitz, D. I.; Marchler, G. H.; Song, J.

S.; Thanki, N.; Yamashita, R. A.; Yang, M.; Zhang, D.; Zheng, C.; Lanczycki, C. J.; Marchler-Bauer, A. CDD/SPARCLE: The Conserved Domain Database in 2020. *Nucleic Acids Res.* **2020**, *48* (D1), D265−D268.
(42) Liu, W.; Xie, Y.; Ma, J.; Luo, X.; Nie, P.; Zuo, Z.; Lahrmann, U.; Zhao, Q.; Zheng, Y.; Zhao, Y.; Xue, Y.; Ren, J. IBS: An Illustrator for the Presentation and Visualization of Biological Sequences. *Bioinformatics* **2015**, *31* (20), 3359−3361.
(43) Jumper, J.; Evans, R.; Pritzel, A.; Green, T.; Figurnov, M.; Ronneberger, O.; Tunyasuvunakool, K.; Bates, R.; Žídek, A.; Potapenko, A.; Bridgland, A.; Meyer, C.; Kohl, S. A. A.; Ballard, A. J.; Cowie, A.; Romera-Paredes, B.; Nikolov, S.; Jain, R.; Adler, J.; Back, T.; Petersen, S.; Reiman, D.; Clancy, E.; Zielinski, M.; Steinegger, M.; Pacholska, M.; Berghammer, T.; Bodenstein, S.; Silver, D.; Vinyals, O.; Senior, A. W.; Kavukcuoglu, K.; Kohli, P.; Hassabis, D. Highly Accurate Protein Structure Prediction with AlphaFold. *Nature* **2021**, *596* (7873), 583−589.
(44) Liu, H.; Naismith, J. H. An Efficient One-Step Site-Directed Deletion, Insertion, Single and Multiple-Site Plasmid Mutagenesis Protocol. *BMC Biotechnol.* **2008**, *8* (1), 91.
(45) Bryksin, A. V.; Matsumura, I. Overlap Extension PCR Cloning: A Simple and Reliable Way to Create Recombinant Plasmids. *BioTechniques* **2010**, *48* (6), 463−465.
(46) Mumberg, D.; Müller, R.; Funk, M. Yeast Vectors for the Controlled Expression of Heterologous Proteins in Different Genetic Backgrounds. *Gene* **1995**, *156* (1), 119−122.
(47) Gietz, R. D.; Schiestl, R. H. Quick and Easy Yeast Transformation Using the LiAc/SS Carrier DNA/PEG Method. *Nat. Protoc.* **2007**, *2* (1), 35−37.
(48) Shindo, D.; Oikawa, T. Energy Dispersive X-Ray Spectroscopy. *Anal. Electron Microsc. Mater. Sci.* **2002**, 81−102.
(49) Newbury, D. E.; Ritchie, N. W. M. Is Scanning Electron Microscopy/Energy Dispersive X-ray Spectrometry (SEM/EDS) Quantitative? *Scanning* **2013**, *35* (3), 141−168.
(50) Villahermosa, D.; Christensen, O.; Knapp, K.; Fleck, O. Schizosaccharomyces pombeMutSα and MutLα Maintain Stability of Tetra-Nucleotide Repeats and Msh3 of Hepta-Nucleotide Repeats. *G3: Genes, Genomes, Genet.* **2017**, *7* (5), 1463−1473.
(51) Zhang, H.; Quintana, J.; Ütkür, K.; Adrian, L.; Hawer, H.; Mayer, K.; Gong, X.; Castanedo, L.; Schulten, A.; Janina, N.; Peters, M.; Wirtz, M.; Brinkmann, U.; Schaffrath, R.; Krämer, U. Translational Fidelity and Growth of Arabidopsis Require Stress-Sensitive Diphthamide Biosynthesis. *Nat. Commun.* **2022**, *13* (1), No. 4009.
(52) Sun, J.; Zhang, J.; Wu, F.; Xu, C.; Li, S.; Zhao, W.; Wu, Z.; Wu, J.; Zhou, C.-Z.; Shi, Y. Solution Structure of Kti11p from *Saccharomyces Cerevisiae* Reveals a Novel Zinc-Binding Module. *Biochemistry* **2005**, *44* (24), 8801−8809.
(53) Zimmermann, B.; Schweinsberg, S.; Drewianka, S.; Herberg, F. W. Effect of Metal Ions on High-Affinity Binding of Pseudosubstrate Inhibitors to PKA. *Biochem. J.* **2008**, *413* (1), 93−101.
(54) Säbel, C. E.; Neureuther, J. M.; Siemann, S. A Spectrophotometric Method for the Determination of Zinc, Copper, and Cobalt Ions in Metalloproteins Using Zincon. *Anal. Biochem.* **2010**, *397* (2), 218−226.
(55) Taiwo, F. A. Electron Paramagnetic Resonance Spectroscopic Studies of Iron and Copper Proteins. *Spectroscopy* **2003**, *17* (1), 53−63.
(56) Mayer, K.; Mundigl, O.; Kettenberger, H.; Birzele, F.; Stahl, S.; Pastan, I.; Brinkmann, U. Diphthamide Affects Selenoprotein Expression: Diphthamide Deficiency Reduces Selenocysteine Incorporation, Decreases Selenite Sensitivity and Pre-Disposes to Oxidative Stress. *Redox Biol.* **2019**, *20*, 146−156.
(57) Argüelles, S.; Camandola, S.; Cutler, R. G.; Ayala, A.; Mattson, M. P. Elongation Factor 2 Diphthamide Is Critical for Translation of Two IRES-Dependent Protein Targets, XIAP and FGF2, under Oxidative Stress Conditions. *Free Radical Biol. Med.* **2014**, *67*, 131−138.
(58) Kroczynska, B.; Blond, S. Y. Cloning and Characterization of a New Soluble Murine J-Domain Protein That Stimulates BiP, Hsc70 and DnaK ATPase Activity with Different Efficiencies. *Gene* **2001**, *273* (2), 267−274.
(59) Zhang, J.; Bai, Z.; Ouyang, M.; Xu, X.; Xiong, H.; Wang, Q.; Grimm, B.; Rochaix, J.; Zhang, L. The DnaJ Proteins DJA6 and DJA5 Are Essential for Chloroplast Iron−Sulfur Cluster Biogenesis. *EMBO J.* **2021**, *40* (13), No. e106742, DOI: 10.15252/embj.2020106742.
(60) Xu, X. M.; Lin, H.; Latijnhouwers, M.; Møller, S. G. Dual Localized AtHscB Involved in Iron Sulfur Protein Biogenesis in Arabidopsis. *PLoS One* **2009**, *4* (10), No. e7662.
(61) Leaden, L.; Busi, M. V.; Gomez-Casati, D. F. The Mitochondrial Proteins AtHscB and AtIsu1 Involved in Fe−S Cluster Assembly Interact with the Hsp70-Type Chaperon AtHscA2 and Modulate Its Catalytic Activity. *Mitochondrion* **2014**, *19*, 375−381.
(62) Couturier, J.; Touraine, B.; Briat, J.-F.; Gaymard, F.; Rouhier, N. The Iron-Sulfur Cluster Assembly Machineries in Plants: Current Knowledge and Open Questions. *Front. Plant Sci.* **2013**, *4*, No. 259.
(63) Fasolo, J.; Sboner, A.; Sun, M. G. F.; Yu, H.; Chen, R.; Sharon, D.; Kim, P. M.; Gerstein, M.; Snyder, M. Diverse Protein Kinase Interactions Identified by Protein Microarrays Reveal Novel Connections between Cellular Processes. *Genes Dev.* **2011**, *25* (7), 767−778.
(64) Popescu, S. C.; Popescu, G. V.; Bachan, S.; Zhang, Z.; Gerstein, M.; Snyder, M.; Dinesh-Kumar, S. P. MAPK Target Networks in *Arabidopsis Thaliana* Revealed Using Functional Protein Microarrays. *Genes Dev.* **2009**, *23* (1), 80−92.
(65) Butković, A.; González, R.; Rivarez, M. P. S.; Elena, S. F. A Genome-Wide Association Study Identifies *Arabidopsis Thaliana* Genes That Contribute to Differences in the Outcome of Infection with Two Turnip Mosaic Potyvirus Strains That Differ in Their Evolutionary History and Degree of Host Specialization. *Virus Evolution* **2021**, *7* (2), No. veab063.
(66) Li, G.; He, Y.; Liu, H.; Liu, D.; Chen, L.; Luo, Y.; Chen, L.; Qi, L.; Wang, Y.; Wang, Y.; Wang, Y.; Zhan, L.; Zhang, N.; Zhu, X.; Song, T.; Guo, H. DNAJC24 Is a Potential Therapeutic Target in Hepatocellular Carcinoma through Affecting Ammonia Metabolism. *Cell Death Dis.* **2022**, *13* (5), No. 490.
(67) Wei, H.; Xiang, L.; Wayne, A. S.; Chertov, O.; FitzGerald, D. J.; Bera, T. K.; Pastan, I. Immunotoxin Resistance via Reversible Methylation of the DPH4 Promoter Is a Unique Survival Strategy. *Proc. Natl. Acad. Sci. U.S.A.* **2012**, *109* (18), 6898−6903.
(68) Hruz, T.; Laule, O.; Szabo, G.; Wessendorp, F.; Bleuler, S.; Oertle, L.; Widmayer, P.; Gruissem, W.; Zimmermann, P. Genevestigator V3: A Reference Expression Database for the Meta-Analysis of Transcriptomes. *Adv. Bioinf.* **2008**, *2008*, 1−5.
(69) Winter, D.; Vinegar, B.; Nahal, H.; Ammar, R.; Wilson, G. V.; Provart, N. J. An "Electronic Fluorescent Pictograph" Browser for Exploring and Analyzing Large-Scale Biological Data Sets. *PLoS One* **2007**, *2* (8), No. e718.
(70) Lill, R.; Mühlenhoff, U. Iron-Sulfur Protein Biogenesis in Eukaryotes: Components and Mechanisms. *Annu. Rev. Cell Dev. Biol.* **2006**, *22* (1), 457−486.
(71) Raut, S.; Yadav, K.; Verma, A. K.; Tak, Y.; Waiker, P.; Sahi, C. Co-Evolution of Spliceosomal Disassembly Interologs: Crowning J-Protein Component with Moonlighting RNA-Binding Activity. *Curr. Genet.* **2019**, *65* (2), 561−573.
(72) Mossessova, E.; Lima, C. D. Ulp1-SUMO Crystal Structure and Genetic Analysis Reveal Conserved Interactions and a Regulatory Element Essential for Cell Growth in Yeast. *Mol. Cell* **2000**, *5* (5), 865−876.
(73) Cao, Y.; Dhahad, H. A.; El-Shorbagy, M. A.; et al. Green synthesis of bimetallic ZnO−CuO nanoparticles and their cytotoxicity properties. *Sci. Rep.* **2011**, *11*, No. 23479.

https://doi.org/10.1021/acsomega.4c01776
ACS Omega 2024, 9, 37650−37661